The use of RUSLE and GCMs to predict potential soil erosion associated with climate change in a monsoon-dominated region of eastern India

Rabin Chakrabortty[1] · Biswajeet Pradhan[2,3,4,5] · Prolay Mondal[6] · Subodh Chandra Pal[1]

Abstract

Soil is one of the most important natural resources; therefore, there is an urgent need to estimate soil erosion. The subtropical monsoon-dominated region also faces a comparatively greater problem due to heavy rainfall with high intensity in a very short time and the presence of longer dry seasons and shorter wet seasons. The Arkosa watershed faces the problem of extreme land degradation in the form of soil erosion; therefore, the rate of soil erosion needs to be estimated according to appropriate models. GCM (general circulation model) data such as MIROC5 (Model for Interdisciplinary Climate Research) of CMIP5 (Coupled Model Intercomparison Project Phase 5) have been used to project future storm rainfall and soil erosion rates following the revised universal soil loss equation (RUSLE) in various influential time frames. Apart from that, different satellite data and relevant primary field-based data for future prediction were considered. The average annual soil erosion of Arkosa watershed ranges from < 1 to > 6 t/ha/year. The very high (> 6 t/ha/year) and high (5–6 t/ha/year) soil loss areas are found in the southern, south-eastern, and eastern part of the watershed. Apart from this, low (1–2 t/ha/year) and very low (< 1 t/ha/year) soil loss areas are associated with the western, northern, southern, and major portion of the watershed. Extreme precipitation rates with high kinetic energy due to climate change are favorable to soil erosion susceptibility. The results of this research will help to implement management strategies to minimize soil erosion by keeping authorities and researchers at risk for future erosion and vulnerability.

Keywords Land degradation · Soil erosion · Climate change · GCM · RCP scenario

✉ Subodh Chandra Pal
geo.subodh@gmail.com

Rabin Chakrabortty
rabingeo8@gmail.com

Biswajeet Pradhan
Biswajeet24@gmail.com; Biswajeet.Pradhan@uts.edu.au

Prolay Mondal
mon.prolay@gmail.com

1   Department of Geography, The University of Burdwan, Bardhaman, West Bengal 713104, India

2   Centre for Advanced Modelling and Geospatial Information Systems (CAMGIS), Faculty of Engineering and IT, University of Technology Sydney, Sydney, NSW 2007, Australia

3   Department of Energy and Mineral Resources Engineering, Sejong University, Choongmu-gwan, 209 Neungdong-ro Gwangjin-gu, Seoul 05006, Korea

4   Center of Excellence for Climate Change Research , King Abdulaziz University , P.O. Box 80234, Jeddah 21589, Saudi Arabia

5   Earth Observation Center Institute of Climate Change, Universiti Kebangsaan Malaysia, Bangi 43600 UKM Selangor, Malaysia

6   Department of Geography, Raiganj University, Uttar Dinajpur, West Bengal 733134, India

Introduction

Soil erosion caused by water action has become one of the most serious issues in the world (Oldeman et al. 1990; Lal 2017). It can remove topsoil or fertile soil from the surface of the earth, and, at the same time, it may reduce the fertility of the soil, which may lead to soil degradation (Stoorvogel et al. 2017; Keesstra et al. 2018). This decline in fertility is economically and ecologically harmful to the entire region. As population pressure is rapidly increasing, deforestation, overgrazing, intensive subsistence agriculture, etc. may become the main causes of soil erosion and degradation (Blaikie 2016; Chakrabortty et al. 2020).

Soil erosion caused by the action of water is a complex occurrence that can be calculated by a number of factors, such as rainfall, soil texture, slope, land use/land cover, and support practice (Panagos et al. 2012). Specifically, various erosion

causal factors and conservation measures determine the direction and amount of water erosion in the area (Thomas et al. 2018). Soil erosion is one of the acute problems of the tropical and subtropical environments, and the amount of erosion is driven by different environmental components (Wischmeier and Smith 1958; Renard et al., 1997; Pal and Chakrabortty 2019a). The amount of soil erosion is a barrier to agricultural productivity as well as proper land and water management (Roy et al. 2020a). In India, half of the land is associated with a high soil erosion zone compared with the tolerance limit (Kumar 2019; Pal and Chakrabortty 2019b).

Human intervention in the natural environment, such as expansion of agricultural activities, deforestation, and conversion of land use practices, may increase the rate of soil erosion (Pal and Shit 2017). The rate of soil erosion can reduce agricultural productivity and increase the rate of sedimentation (Gebrernichael et al. 2005; Wang et al. 2012). Increased sedimentation rates are a major challenge in the subtropical region (Pal and Chakrabortty 2019b; Saha et al. 2020). It reduces the life span of the reservoir, which is considered a major economic problem for third world countries such as India (Carley and Christie 2017). In this region, there is a large dependence on agricultural productivity, which is increasing in quantity every day to meet the needs of the growing population. The conversion of vegetative land into agricultural land plays a key role in the susceptibility of soil erosion in this region. There is a clear cut effect of soil erosion and associated sedimentation between the carbon of the atmosphere and the soil (Lal 2005). Numerous models in different disciplines have been considered in different regional scales to predict soil erosion and associated sedimentation when considering the availability of the necessary records to calibrate the models (Lal 2001; Zeng et al. 2017; Toubal et al. 2018; Arabameri et al. 2020).

Various types of empirical models are available for estimating soil erosion and are usable in a different environment with little modification (Lane et al. 1997). Both the revised universal soil loss equation (RUSLE) and USLE are applicable to the estimation of the average erosion rate in the geographic information system (GIS) environment and are capable of determining the spatial difference in soil loss (Prasannakumar et al. 2012; Bera 2017; Senanayake et al. 2020). RUSLE is one of the reliable techniques that can be applied in tropical and subtropical areas and even in forest-dominated watersheds (Biswas and Pani 2015). Apart from these different empirical and semi-empirical methods, multi-criteria analysis is an important method that can be used by considering the importance of different themes and their related sub-themes (Pal 2016; Hembram and Saha 2020). Local knowledge of the stakeholder is essential in terms of soil loss and related problems. For this purpose, Shit et al. (2015) investigated farmers' perceptions of land losses and determined that management strategies are meaningful, although there are some spatial differences. Biologic activity also increases the

potential for soil erosion. The root density of plants increases soil erodibility (De Baets et al. 2006).

C (cover and management factor) is one of the most important factors in the RUSLE model, which is the effect of vegetation and land use/land cover (Karaburun 2010; Ganasri and Ramesh 2016). The C factor represents the importance of vegetation cover and associated management practices for soil loss (Morgan et al. 1998; Gomez et al. 2009). This factor deals with management strategies to reduce soil erosion by adopting various soil-related measures (Van der Knijff et al. 2000). Traditional measures could generally be seen as part of strategies to manage soil erosion in subtropical regions. Land degradation from soil erosion is currently considered to be a monotonous situation that is directly linked to the decline in agricultural productivity and, on the other hand, increases the rate of sedimentation in the reservoir. Most countries in the world are mainly dependent on the growth of agriculture and its related activities.

The potential impact of climate variability on soil loss is clear to researchers (Zhang and Nearing 2005). Rainfall and runoff erosion factors are the most important factor in the subtropical region and are capable of estimating the impact of rainfall on soil erosion (Gupta and Kumar 2017). It has been observed that there is an upward trend in the simulated rainfall scenario in most of the region worldwide. This upward trend of the simulated rainfall scenario is crucial for soil erosion assessment, given that most of the subtropical regions face extreme soil erosion due to storm rainfall (Edwards and Owens 1991). Rainfall and runoff (R) are the most important factors for soil erosion in the subtropical region. It is therefore necessary to identify its nature in the future period in order to predict future soil erosion in the region. The general circulation model (GCM) predicted that both temperature and rainfall patterns (severity and frequency) would continue to increase (Roy et al. 2020b). In the twenty-first century, most regions of India have to face extreme weather–related events (Malik et al. 2020). Major impacts of the climate change scenario has been projected, and multiple studies predict an upward trend of rainfall scenario and associated soil loss in different parts of the world. The potential impact of climate change on soil erosion in this region has not been studied in the past. So, we simulated the R factor as a dynamic component of soil erosion modeling to predict the amount of soil erosion up to the twenty-first century. The overall region is dependent on the subsistence-based agricultural practices. So, the potential impact of climate change and its associated extreme climatic condition can help the policymakers to take proper step for sustainable land management practices.

Remote sensing and the GIS technique have become useful for estimating soil erosion in the catchment area (Pal and Shit 2017). The Arkosa watershed of the Dwarkeswar River Basin in India is selected as a study area for quantifying the amount of soil loss associated with the "revised universal soil loss equation" method and the GIS technique. The pixel-wise

value of all factors (R, K, LS, C, and P) was then worked out as a data format in the GIS environment. Most of the soil erosion study is associated with quantifying the rate of erosion, but there is no potential impact due to climate change in the future. The likely impact of extreme rainfall scenarios on the assessment of future potential soil loss areas is associated with this study. This type of information is very useful for planning purposes, in particular the management of the watershed, the establishment of a check dam to reduce the rate of sedimentation, and so on in a precise way. The objective of this study is to determine whether the impact of simulated precipitation is responsible for soil erosion and what measures and practices are needed for land use in order to reduce the risk and protect the soil.

Study area

The Arkosa watershed is an important watershed of the Dwarkeswar River Basin and is located in the West Bengal Bankura District (Fig. 1). The latitudinal and longitudinal extension of this watershed is 23° 9′ 49″ N to 23° 20′ 24″ N and 86° 37′ 48″ E to 86° 54′ 53″ E with an area of 34,852 ha (Pal and Chakrabortty 2019a). The Arkosa river originates from the eastern part of the Purulia District and meets the Dwarkeswar River in the Bankura District of West Bengal. In the Indian Watershed Atlas, the watershed code is 2A2C8 (Pal and Chakrabortty 2019a). The Dwarkeswar River originates from Panjoniya or Dunghru Hill of Purulia District and then enters into the Bankura District near Chhatna C.D. Block (Chakrabortty et al. 2018).

Database and methodology

The data mainly contains the average annual soil loss (ton/ha/year) of Arkosa watershed using the "revised universal soil loss equation" in the GIS environment (Abu Hammad 2011) (Table 1). The data consists of the primary data collected and generated by using the SRTM (Shuttle Radar Topographic
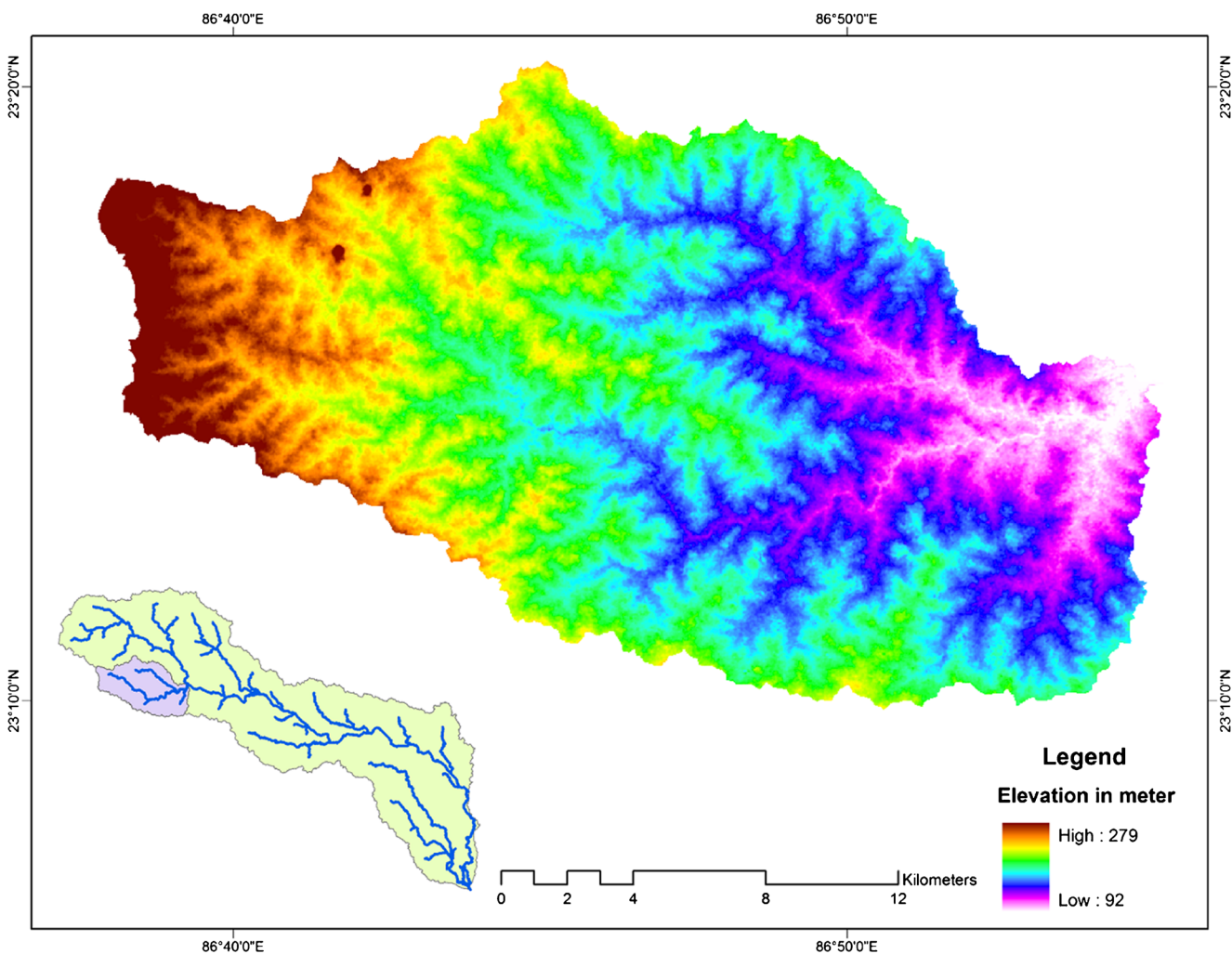

Fig. 1 Location of the study area

Table 1 Specification table

Subject area	Geography
Specific subject area	Pedo-geomorphology
Type of data	Table and figure
Data acquired	Primary data as well as acquired from GIS approaches
Experimental factors	All the parameters are derived from the empirical equation in different published materials.
Experimental parameters	Estimation of soil erosion using RUSLE model in GIS environment of Arkosa watershed in Dwarkeswar River Basin
Location	The latitudinal and longitudinal extension is 23° 9′ 49″ N to 23° 20′ 24″ N and 86° 37′ 48″ E to 86° 54′ 53″ E with an area of 34,852 ha
Data accessibility	All types of data are associated in this article

Mission), the digital elevation model (DEM), and the Landsat 8 OLI satellite image, incorporating the various empiric equations in the GIS environment (Eqs. 1–10) (Fig. 2). Average annual soil loss derived from RUSLE with regard to "rainfall and runoff erosivity factor" (R), "soil erodibility factor" (K), "slope length and steepness factor" (LS), "coverage and management factor" (C), and "support slope direction practice factor" (P) in the GIS environment (Pal and Shit 2017).

In this study, the "RUSLE" method is considered to estimate the amount of soil loss to the Dwarkeswar River Basin in the GIS environment. This erosion model can be used to estimate soil erosion caused by water action. The RUSLE factors can also highlight the impact of rainfall, soil, topography, land use/land cover, related support practices, etc. (Pal and Shit 2017). The "rainfall and runoff erosivity factor" was estimated from the primary rainfall experience at different rain gauge stations during the rainfall season (Pal and Chakrabortty 2019). Grid-wise soil samples were collected, and their texture and chemical properties were analyzed in order to estimate the

soil erosion factor. The slope and flow accumulation derived from SRTM and DEM have been prepared for the assessment of the "slope length and steepness factor" in the GIS environment (Pal and Chakrabortty 2019b). The NDVI (normalized difference vegetation index) has been prepared as a reliable vegetation algorithm for the "cover and management factor" process. The correlation between the C factor and the NDVI is positively high. The support practice factor related to the amount and direction of the slope was prepared on the basis of the information observed during the field survey in the Arkosa watershed. The "revised universal soil loss equation" was taken into consideration for estimating the average annual soil loss (Chakrabortty et al. 2018) of Arkosa watershed:

$$A = R \times K \times LS \times C \times P \qquad (1)$$

where, A is the "average annual soil erosion" (ton/ha/year), R is the "rainfall and runoff erosivity factor" (MJ mm/ha/h/year), K is the "soil erodibility factor" (ton/ha), LS is the "slope

Fig. 2 Methodology flow chart
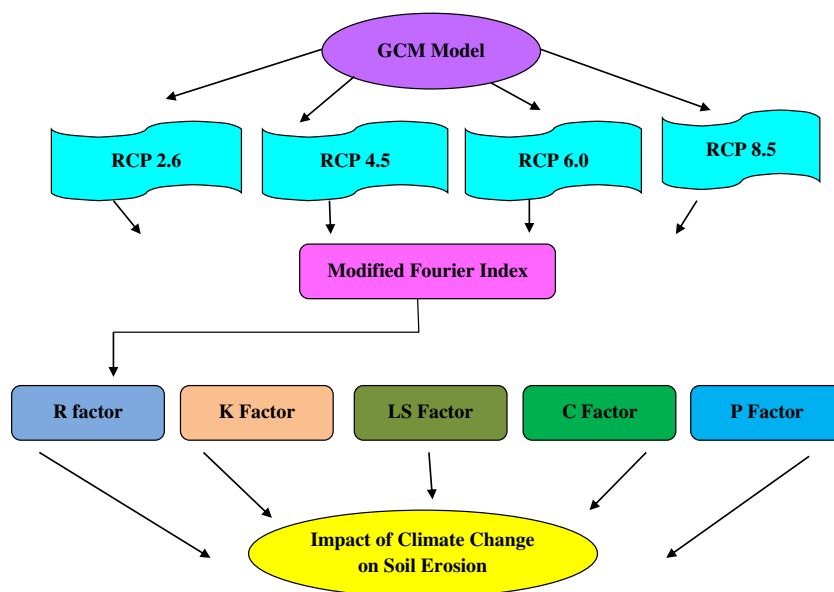
length and steepness factor," C is the "cover and management factor," and P is the support practice factor (Pal and Chakrabortty 2019a).

Rainfall and runoff erosivity factor

The "rainfall and runoff erosivity" (R) factor shows that erosivity occurred due to rainfall and runoff in the watershed. There is a positive relationship between the rainfall and the amount of R. The value of the R factor is calculated from the long-term weekly rainfall record collected. The R factor of the Arkosa watershed is shown here in MJ mm/ha/h/year (Arnoldus 1980). The following methods have been taken into account for estimating the different factors in the GIS environment:

$$R = \sum_{i=0}^{12} 1.735 \times 10^{\left(1.5\log_{10}\left(\frac{P_i^2}{P}\right) - 0.08188\right)} \tag{2}$$

where R is the rainfall and runoff erosivity factor, and it expresses in MJ/ha/year (Arnoldus 1980).

Soil erodibility factor

The "soil erosion factor" (K) is defined as the general soil erosion capacity. Generally, surface soil confrontation due to precipitation raindrops on exposed soil surfaces is demonstrated. Here, K is an influential factor in soil erosion, which is determined experimentally by considering the different physical and chemical properties of soil as well as soil texture, soil structure, permeability, and content of organic matter (Wischmeier et al. 1971). RUSLE calculates the factor of spatial soil erosion in the GIS environment. For each soil type, the K factor was calculated from soil samples collected during empirical field observation and laboratory experiments. The map of the K factor is then classified to show the variation in erodibility within the Arkosa watershed. The soil factor K has been calculated using Eq. 3 (Teng et al. 2018):

$$K = 0.0137 \times \left(0.2 + 0.3 \times e^{\left[-0.0256 \times San \times \left(\frac{1-Sil}{100}\right)\right]}\right)$$
$$\times \left(\frac{Sil}{Cla + Sil}\right)^{0.3} \times \left[1 - \frac{0.25 \times TOC}{TOC + e^{(3.72 - 2.95 \times TOC)}}\right]$$
$$\times \left[1 - \frac{0.7 \times SN_1}{SN_1 + e^{(22.9 \times SN_1 - 5.51)}}\right] \tag{3}$$

where K is the soil erodibility, San is the percentage of sand, Sil is the percentage of silt, Cla is the percentage of clay, and SN_1 is the 1-San/100.

Slope length and steepness factor

In RUSLE, two factors are mainly responsible for the ruggedness of the overall topography, namely, the slope length factor (L) and the steepness factor (S), which are responsible for the erosion of the surface soil (Yang et al. 2003). The slope length and steepness factor (LS) is a specific method for combining the impact of the slope length and its steepness (Panagos et al. 2015). The LS factor is related to the percentage of slope and length of slope defined as the ratio of soil loss between slope steepness and slope length under a specific condition (Van Remortel et al. 2004). The higher LS values indicate the very high potential for erosion and its associated risk. Here, the LS factor is estimated by incorporating both L and S into a single framework and the GIS platform with the help of Eqs. 4 and 5 (Moore and Burch 1986):

$$LS = (m+1) \times \left[\frac{A_s}{22.}\right] \times \left[\frac{sin\beta}{0.0896}\right] \tag{4}$$

$$A_s = \frac{1}{b_1} \sum_{i=1}^{N} a_1 u_1 \tag{5}$$

where LS is the length of the slope and the steepness factor, the length of the slope in meter, and β is the angle of the slope (Van Romortel et al. 2001).

Cover and management factor

The management factor (C) covers the impact of farming practices as well as the management strategies adopted with regard to soil erosion. Here, the C factor shows how specific management strategies address the impact of soil erosion on the watershed. The vegetation generally protects the exposed soil surface from the energy of rain before it reaches the surface of the soil (Pimentel 2006; Neave and Rayburg 2007). Therefore, the C factor has become an important parameter for assessing soil erosion and is evidently computed following experiential equations related to field vegetation information (Wischmeier 1978). Several researchers used several methods to calculate the C factor following the NDVI values for soil erosion in the GIS environment (Van der Knijff et al. 2000). The NDVI is the most reliable vegetation index and is widely used in various disciplines to estimate the amount of vegetation (Pal et al. 2018; Malik et al. 2019). The NDVI was estimated from Eq. 6 (Rouse Jr 1974):

$$NDVI = \frac{(NIR - Red)}{(NIR + Red)} \tag{6}$$

The exponential function of the NDVI algorithm is then considered for the estimation of the C factor raster in the GIS environment (Zhou et al. 2008; Kouli et al. 2009):

$$C = exp\left[-a\frac{\mathrm{NDVI}}{(\beta-\mathrm{NDVI})}\right] \qquad (7)$$

where a and β are units with fewer parameters capable of estimating the curve between NDVI and its associated C factor. This scenario provides an exponential improvement in predictability over linear association (Van der Knijff et al. 2000).

Support practice factor

The "support practice factor" (P) is the proportion of soil erosion between accurate support practices and similar upper and lower slopes. The P factor was estimated on the basis of various management practices based on the slope direction observed during the field visit. The observed empirical information on support and management practices has been considered in this study.

Rainfall and runoff erosion is one of the most important factors in soil erosion. Rainfall has a significant impact on soil erosion susceptibility in subtropical monsoon climates. The most vulnerable to soil erosion is the correspondence between a long dry season and a short rainy season with high rainfall intensity. The amount and intensity of rainfall during this period are very high.

Here, long-term historical GCM data (1900–2000) with observed data during the same period were considered. Statistical downscaling approaches have been considuish in a systematic way. Here, we distinguish between monsoon period records and the recorded data from the downscaled GCM data. Various models were considered for GCM data in order to assess the accuracy of the GCM and to select appropriate GCM data. Here, the most suitable GCM data is the "Model for Interdisciplinary Research on Climate"(MIROC5) of the "Coupled Model Intercomparison Project" (CMIP5) climate model. Average bias between model data and observed data was then considered for the simulation of future precipitation (RCP 2.6, RCP 4.5, RCP 6.0, and RCP 8.5). Removing the marginal error, we considered the different influential timeframes (5, 10, and 15 years). The rainfall of the monsoon period in historical, observed, and future periods was considered in this study. Rainfall scenarios have been taken into account here to approximate the "rainfall and runoff erosivity factor" in the forecast period.

In particular, some errors are associated with GCM data which are not capable of calculating the exact precipitation scenario. Consequently, the key function for modeling a scenario is to eliminate bias by using appropriate techniques. The information observed is considered to eliminate bias and to be assigned to the control or historical period in the time of the scenario. For this reason, using the following formula, the technique of natural breaks is considered to be the form and

size feature in the likelihood function while using α and β (Shrestha and Lohpaisankrit 2017; Mishra et al. 2018; Nyaupane et al. 2018).

$$X_{\mathrm{GCM_{Present-Corrected}}} = F_{obs}{}^{-1}(F_{\mathrm{GCM_{Present}}}(X_{\mathrm{GCM20_{Present}}})) \qquad (8)$$

$$X_{\mathrm{GCM_{Future-Corrected}}} = X_{\mathrm{GCM_{Future}}}$$

$$= \frac{F_{Obs}{}^{-1}(F_{\mathrm{GCM_{Future}}}(X_{\mathrm{GCM_{Future}}}))}{F_{\mathrm{GCM_{Present}}}{}^{-1}\left(F_{\mathrm{GCM_{Future}}}(X_{\mathrm{GCM_{Future}}})\right)} \qquad (9)$$

$$f(X) = \frac{1}{\beta^\alpha \tau(\alpha)} X^{\alpha-1} \exp\frac{X}{\alpha} \qquad (10)$$

$$F(X) = \int_0^x f(t)dt \qquad (11)$$

The results of the various points were then interpolated with the consideration of spatial interpolation techniques in the GIS environment with a view to estimating and using spatial variations in soil erosion.

We estimated the predictable rainfall and runoff erosivity factor when considering the MFI ("modified Fourier index") for the elimination of rainfall limitations and the elimination of exponential relationships (Pal and Chakrabortty 2019b) in the following way:

$$\mathrm{FI} = \frac{P^2 \max}{P} \qquad (12)$$

$$\mathrm{MFI} = \sum_{i=1}^{i=12} \frac{P^2 1}{P} \qquad (13)$$

The simulated rainfall and runoff erosivity factor was taken into account when considering the modified Fourier index (Plangoen et al. 2013; Tiwari et al., 2016; Pal and Chakrabortty 2019b):

$$R = a\mathrm{MFI}^b + \varepsilon \qquad (14)$$

Here are the parameters a and b, which are estimated in an empirical way, and ε is the normal error (Plangoen et al. 2013; Tiwari et al., 2016; Pal and Chakrabortty 2019b).

Results and discussion

This watershed has unique characteristics in terms of geological, geomorphic, hydro-geomorphic, and pedo-geomorphic conditions. The undulating lateral topography with occasional hills, sloping strips, and high rainfall intensity during the wet season causes high erosion. Apart from this, the combination of a long dry season and a short rainfall span with a high quantity is most favorable to soil loss.

The rainfall and runoff erosive factor is the capacity of storm rainfall for soil material erosion. In the monsoon-dominated region, the presence of seasonality and a short span
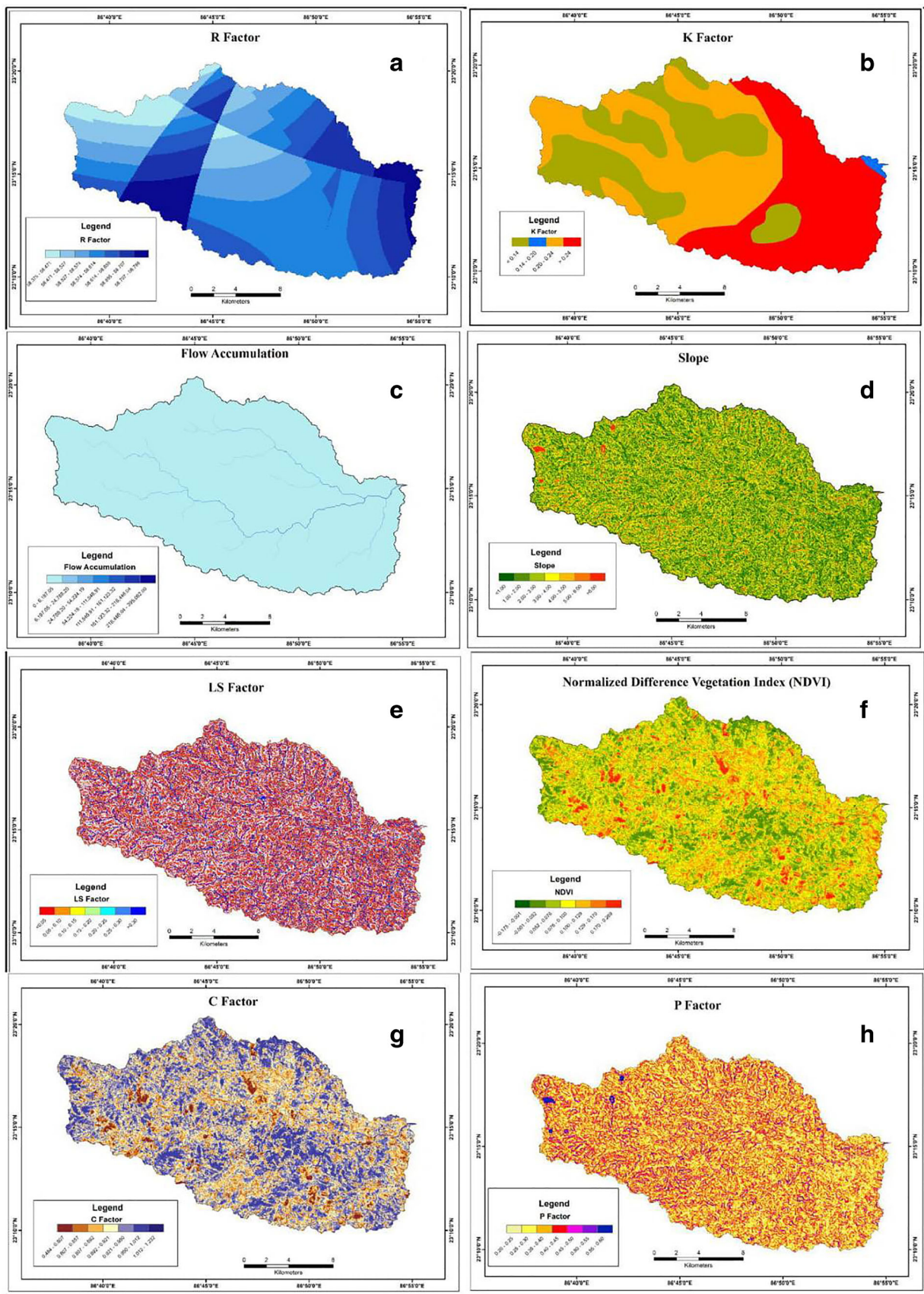
Fig. 3 *R* factor (**a**). *K* factor (**b**). Slope (**c**). Flow accumulation (**d**). *LS* factor (**e**). NDVI (**f**). *C* factor (**g**). *P* factor (**h**)

Table 2 Factor-wise areal coverage of Arkosa watershed

Factors	Class name	Class range	Area in hectare	Area in %
R factor	Very high	58.707–58.798	3938.276	11.300
	High	58.655–58.707	3380.644	9.700
	Moderately high	58.614–58.655	3206.384	9.200
	Moderate	58.574–58.614	12,930.092	37.100
	Moderately low	58.527–58.574	3101.828	8.900
	Low	58.471–58.527	2927.568	8.400
	Very low	58.375–58.471	5367.208	15.400
K factor	Very high	> 0.24	14,812.100	42.500
	High	0.20–0.24	10,420.748	29.900
	Moderate	0.14–0.20	7911.404	22.700
	Low	< 0.14	1707.748	4.900
Slope	Very high	> 6	3345.792	9.600
	High	5–6	1638.044	4.700
	Moderately high	4–5	2369.936	6.800
	Moderate	3–4	9131.224	26.200
	Moderately low	2–3	4705.020	13.500
	Low	1–2	6064.248	17.400
	Very low	< 1	7597.736	21.800
Flow accumulation	Very high	218,446.04–395,062.00	421.709	1.210
	High	161,123.32–218,446.04	236.994	0.680
	Moderately high	111,546.91–161,123.32	181.230	0.520
	Moderate	54,224.19–111,546.91	149.864	0.430
	Moderately low	24,788.20–54,224.19	170.775	0.490
	Low	6197.05–24,788.20	216.082	0.620
	Very low	0–6197.05	33,475.346	96.050
LS factor	Very high	> 0.30	7911.404	22.700
	High	0.25–0.30	3206.384	9.200
	Moderately high	0.20–0.25	2997.272	8.600
	Moderate	0.15–0.20	3276.088	9.400
	Moderately low	0.10–0.15	2056.268	5.900
	Low	0.05–0.10	2335.084	6.700
	Very low	< 0.05	13,069.500	37.500
NDVI	Very high	0.176–0.269	3624.608	10.400
	High	0.129–0.176	2369.936	6.800
	Moderately high	0.100–0.129	1847.156	5.300
	Moderate	0.076–0.100	15,927.364	45.700
	Moderately low	0.052–0.076	2857.864	8.200
	Low	− 0.001−− 0.052	2753.308	7.900
	Very low	− 0.175−− 0.001	5471.764	15.700
C factor	Very high	1.012–1.232	4042.832	11.600
	High	0.950–1.012	2631.326	7.550
	Moderately high	0.921–0.950	2387.362	6.850
	Moderate	0.892–0.921	14,812.100	42.500
	Moderately low	0.857–0.892	3188.958	9.150
	Low	0.807–0.857	2753.308	7.900
	Very low	0.484–0.807	5036.114	14.450
P factor	Very high	0.55–0.60	4359.985	12.510
	High	0.50–0.55	1690.322	4.850
	Moderately high	0.45–0.50	2509.344	7.200

Table 2 (continued)

Factors	Class name	Class range	Area in hectare	Area in %
	Moderate	0.40–0.45	3087.887	8.860
	Moderately low	0.35–0.40	5670.420	16.270
	Low	0.30–0.35	6548.691	18.790
	Very low	0.25–0.30	10,985.350	31.520

of high rainfall intensity results in high erosion potential (Pal and Chakrabortty 2019b). Here, the weekly average rainfall record is associated with the same units to determine the R factor. The R factor values of this region range from 58.375 to 58.798 MJ mm ha^{-1} year^{-1} (Fig. 3a). The very high R factor values (58.707–58.798) are concentrated in the northern, south-western, and eastern portions of the watershed. Apart from this, most of the areas are associated with high (58.655–58.707), moderately high (58.614–58.655), moderate (58.574–58.614), moderately low (58.527–58.574), low, and very low (58.471–58.527) values.

The combination of the different causal properties of the soil influences the process of erosion. The soil has been the result of numerous physical, chemical, and biological conditions over a long period of time. The K factor values of the Arkosa watershed range from 0.14 to 0.24 (Fig. 3b). In this area, the higher K value, which is more prone to erosion, is associated with the lower part. Apart from this, the rest of the area is associated with moderate to low K values, which are less prone to erosion than the lower part of the watershed.

The "slope length and steepness factor" is the capacity of the soil loss potential that is directly related to the topographic characteristics. The kinetic energy, which depends on the amount of slope, is directly related to the gravitational force. In the GIS environment, therefore, the flow accumulation algorithm (Fig. 3c) and the slope raster (Fig. 3d) are the primary determinant of the LS factor estimation. The values of the LS factor of this watershed range between < 0.05 and > 0.30 (Fig. 3e). The western portion (upper portion) has a maximum slope, and the remaining area is associated with a moderate to low LS factor. The maximum amount of flow accumulation is found in the eastern portion, but the soil loss is associated with the amount of active kinetic energy.

The cover and management factor is related to surface cover, which acts as a determining control or prevents soil loss. The amount of surface coverage of any region is not static; it is time to time changeable. Natural control of the cover and management factor is estimated on the basis of a vegetation algorithm. For this purpose, the NDVI has been considered for the assessment of the C factor (Fig. 3f). In the GIS platform, the C factor depends not only on

the amount of vegetation covered but also on the amount of canopy covered, the density, roughness, the amount of bare surface, and also the association between the vegetation cover and the bare surface. This technique is useful in eliminating the possible overlap between the canopy cover and the bare surface. The values of the NDVI range between negative (−) 0.175 and positive (+) 0.269 (Table 2). The C factor of this watershed ranges from 0.484 to 1.232. The high C factor is concentrated in the forest area, and the rest of the area is associated with moderate to low C values (Fig. 3g). Here, we have found a very significant relationship between the C factor and the NDVI raster (Fig. 4).

The support practice factor indicates the proportion of specific support practices. Generally, the support practice and its associated management factor can control the amount of soil loss in a given area. The P factor values were adopted according to the number of support practices initiated by local stakeholders. In this case, the amount of support practices has been incorporated according to the percentage of slope direction. In this region, no specific support practice has been adopted to reduce the amount of soil erosion. Field bundling is a specific type of traditional measures that have been largely implemented in intensive subsistence agricultural regions to control high soil erosion as well as to trap surface runoff;
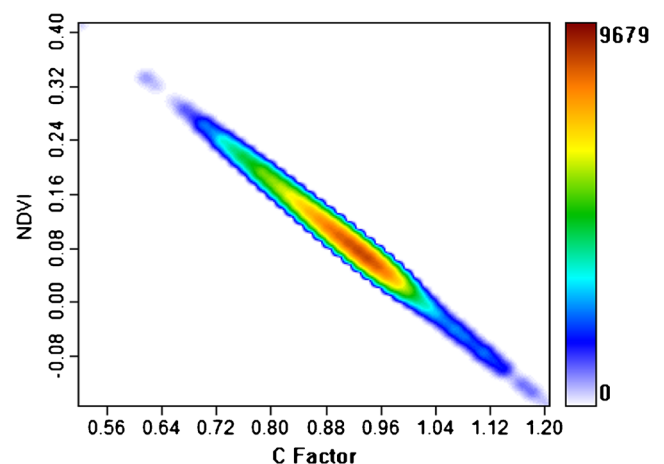

Fig. 4 Correlation between the C factor and NDVI

Table 3 Average annual soil erosion and its areal coverage

	Class name	Class range (ton/ha/year)	Area in hectare	Area in %
Average annual soil loss	Very high	> 6.00	1446.3	4.150
	High	5.00–6.00	2712.6	7.783
	Moderately high	4.00–5.00	2020	5.796
	Moderate	3.00–4.00	3021	8.668
	Moderately low	2.00–3.00	3363.5	9.651
	Low	1.00–2.00	3210	9.210
	Very low	< 1.00	19,078.6	54.742

diversification of land with such traditional practices is also taking place in the tropical and subtropical environments of this watershed. This area is dominated only by paddy cultivation; therefore, a monocropping system has been organized. High *P* factor values have mainly been found in areas where traditional support practices have been adopted, and the soil erosion of this area is low. The other regions are associated with moderate to low *P* factor values, and the potential for soil losses in this area is high (Fig. 3h).

The amount of soil erosion of this region ranged from < 1 to > 6 t/ha/year (Table 3). The output erosion raster was then reclassified into different qualitative classes, taking into account separate threshold units, i.e., 1, 2, 3, 4, 5, and 6 (Fig. 5). The very high soil loss classes (> 6 t/ha/year) are largely confined in the southern and southeastern parts of the watershed. The high soil loss (5–6 t/ha/year) areas are largely confined in the eastern portion of the watershed. The moderately high (4–5 t/ha/year) soil loss areas are largely confined in the eastern and middle
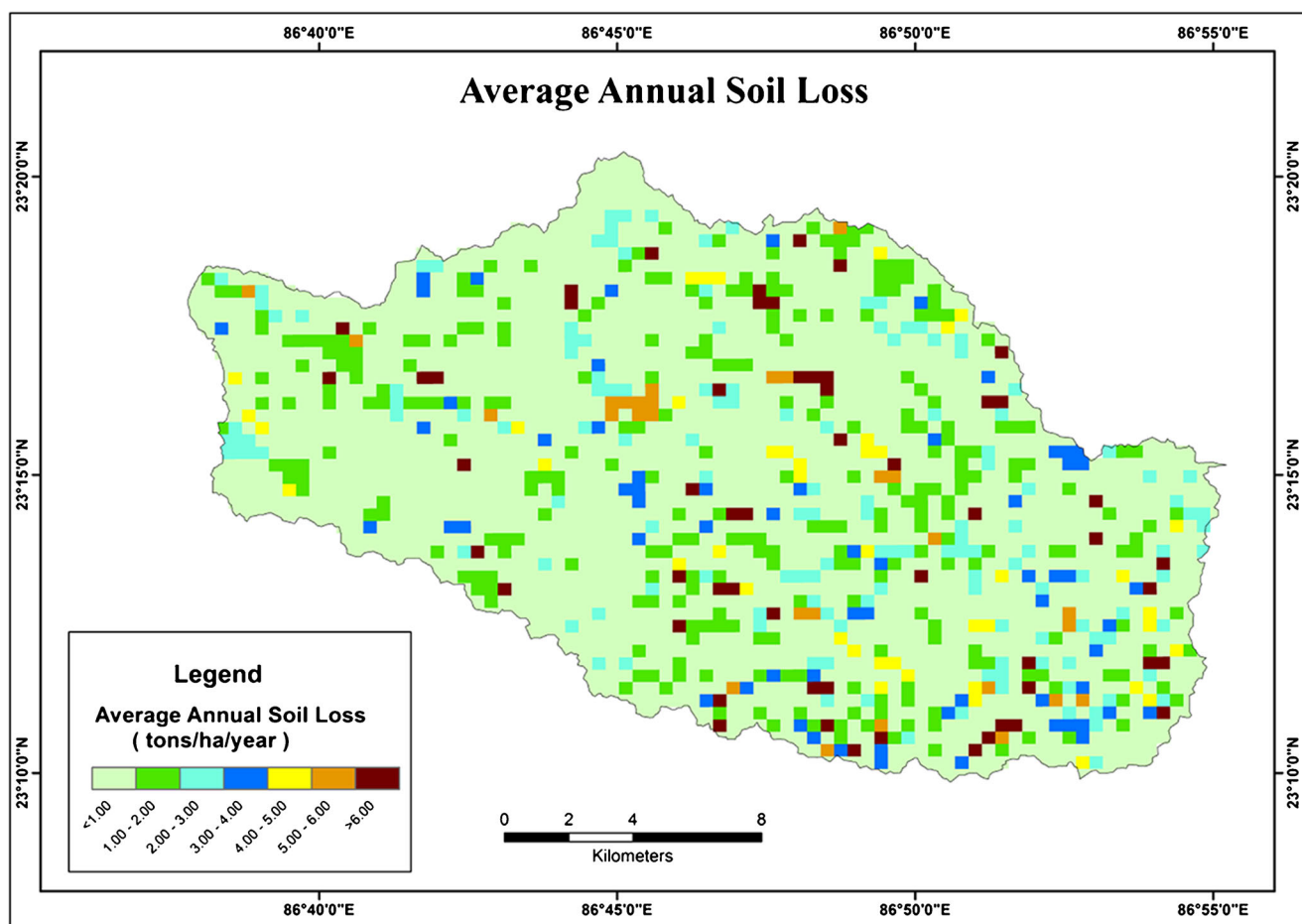
Fig. 5 Average annual soil loss

Fig. 6 Validation of the study and model through measuring the amount of soil deposition near the check dam


parts of the watershed. The medium soil loss (3–4 t/ha/year) areas are mainly concentrated in the south-eastern portion of the watershed (Table 3). The moderately low (2–3 t/ha/year) soil loss areas are mainly found in the eastern part of the watershed. Low (1–2 t/ha/year) soil loss areas are largely confined to the western, northern, and southern parts of the watershed. Very low (< 1 t/ha/year) soil loss areas are mainly found in most locations in the watershed. This type of information may be useful for local stakeholders as well as regional planners to propose the most appropriate development paradigm, taking into account the characteristics of the local environment.

The entire output of this model was validated at the primary sedimentation rate observed for the different gully plug or check dam records. This information is very similar to the model output, which shows the high accuracy (91.43 area under the curve) of the ROC curve (Figs. 6 and 7). It can therefore be argued that this specific model of this area is perfectly suited and should be applied to the subtropical regions of the world.

Various scenarios of RCP (2.6, 4.5, 6.0, and 8.5) were considered to estimate the simulated rainfall status. Here, some variations of RCP wise have been identified. There is a general upward trend in rainfall, both in the future and in the historical, by increasing the RCP scenarios. Some oscillation has been found in the history of storm rainfall (Fig. 8a). Apart from that, we divided the historical records (observed, GCM, and corrected GCM) according to the moving average method (Fig. 8b). In the case of a

simulated future rainfall event, we consider different RCP scenarios with different influential timeframes to minimize the error with respect to the predicted rainfall scenario (Fig. 8c). In RCP 2.6, the values of the rainfall and runoff erosivity factor range from 76.69 to 77.16 in 5-year influential timeframes, 83.51 to 84.56 in 10-year influential timeframes, and 84.51 to 85.70 in 15-year influential timeframes. In RCP 4.5, the values of the rainfall and runoff erosivity factor range from 85.28 to 86.96 in 5-year influential timeframes, 96.60 to 97.91 in 10-year influential timeframes, and 96.97 to 98.48 in 15-year influential
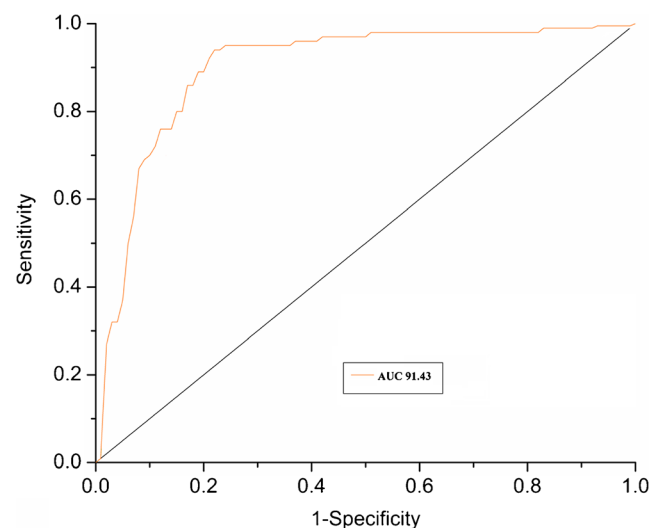
Fig. 7 Validation of the study through ROC curve
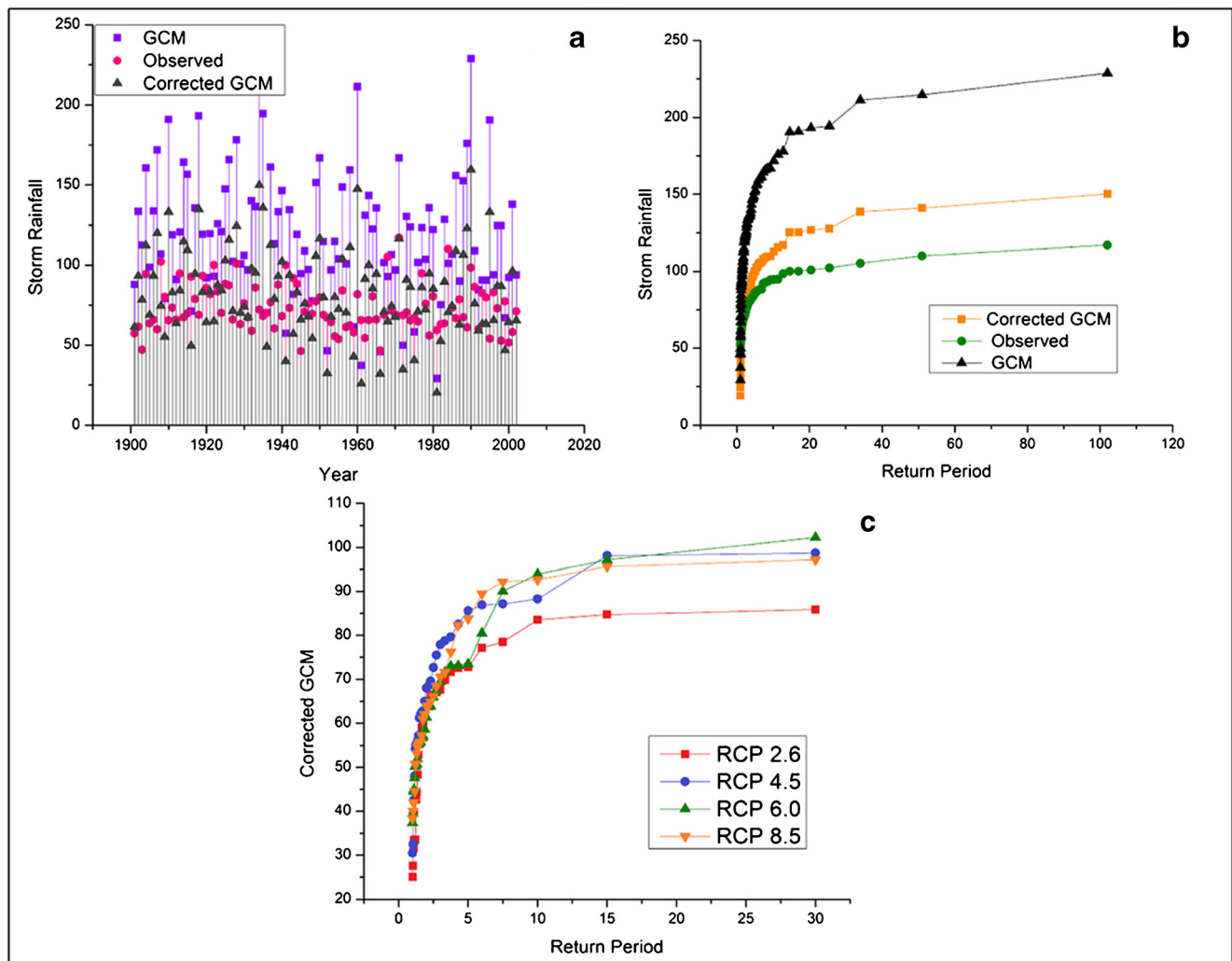
Fig. 8 Year-wise rainfall in historical periods (1900–2000) (**a**). Historical storm rainfall in different influential time frameworks (**b**). Simulated rainfall scenario in different influential time frameworks (**c**)

timeframes (Fig. 9). In RCP 6.0, the values of the rainfall and runoff erosivity factor range from 79.03 to 80.30 in 5-year influential timeframes, 96.05 to 97.02 in 10-year influential timeframes, and 100.68 to 102.03 in 15-year influential timeframes. In RCP 8.5, the values of the rainfall and runoff erosivity factor range from 92.35 to 93.39 in 5-year influential timeframes, 95.59 to 95.69 in 10-year influential timeframes, and 96.80 to 97.12 in 15-year influential timeframes.

This model indicates that the rising propensity of soil erosion is found in the different RCP scenarios. We divided the period with different influential time frameworks for minimizing the probable period. We cannot say the actual amount of precipitation in a particular time. So, the different influential timeframes (5, 10, and 15 years) are a reliable method for projecting the simulated rainfall scenario, which is very much influential on soil erosion susceptibility. We found that the increasing trend of soil erosion has increased in the RCP scenario (Fig. 10). However, there is

some degree of erosion minimization in RCP 6.0 compared with other RCP scenarios. Aerial coverage for simulated soil erosion is shown in Table 4.

Conclusion

The impact of extreme rainfall has had a significant impact on soil erosion during the forecast period. There is a direct impact in this area of monsoon climate and extreme rainfall with high intensity and high kinetic energy. This type of research is therefore helping to identify the direct and indirect impacts of climate change on the soil erosion scenario. In recent times, there has been an increasing tendency to apply geospatial technology to various problems and associated management strategies. It is time-consuming and is dealing with an adequate level of accuracy. Different raster layers have been used to estimate the amount of soil erosion and to estimate the spatial
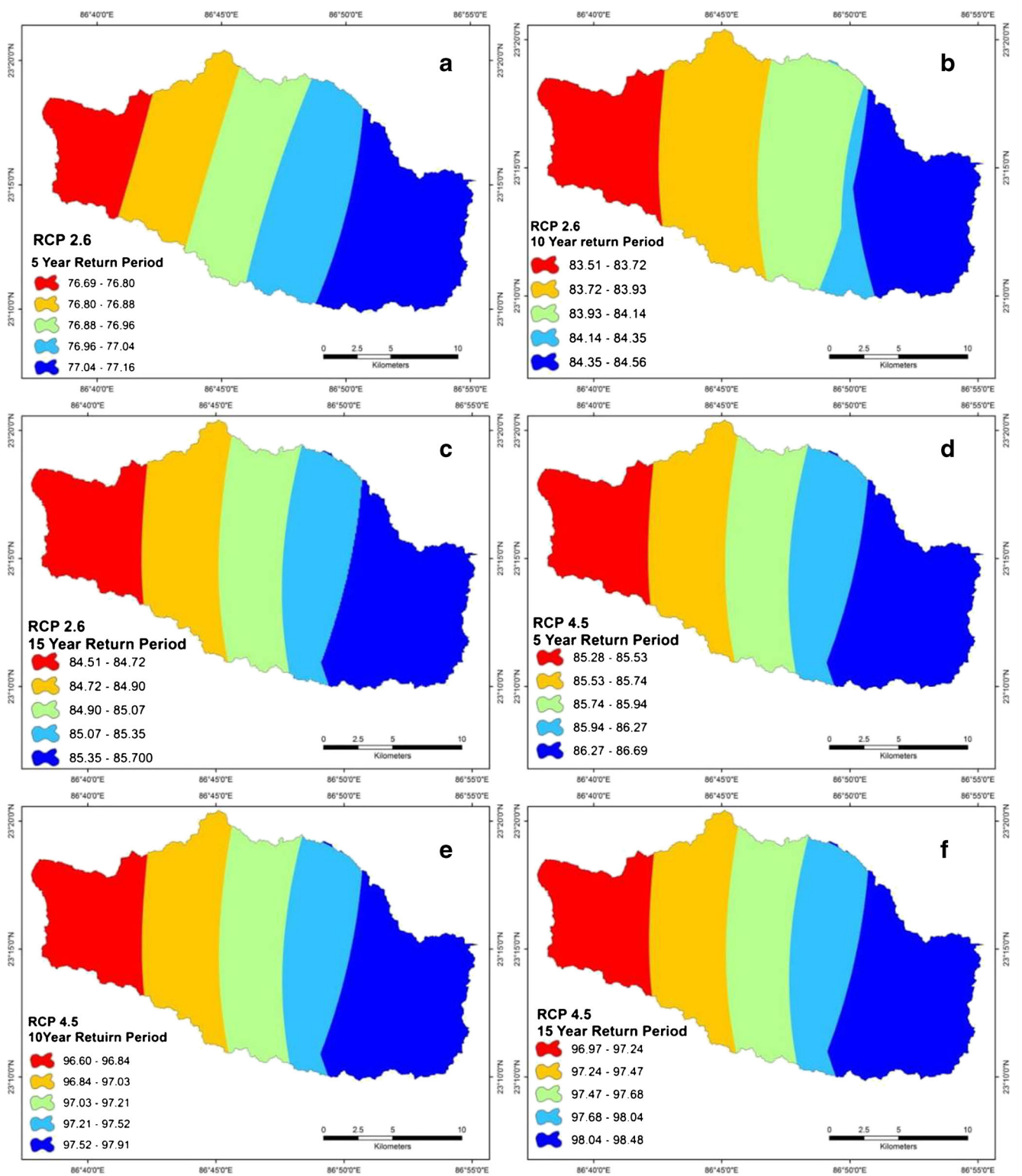
Fig. 9 Future rainfall and runoff erosivity factor. RCP 2.6 in 5-year influential time frameworks (**a**). RCP 2.6 in 10-year influential time framework (**b**). RCP 2.6 in 15-year influential time framework (**c**). RCP 4.5 in 5-year influential time framework (**d**). RCP 4.5 in 10-year influential time framework (**e**). RCP 4.5 in 15-year influential time framework (**f**). RCP 6.0 in 5-year influential time framework (**g**). RCP 6.0 in 10-year influential time framework (**h**). RCP 6.0 in 15-year influential time framework (**i**). RCP 8.5 in 5-year influential time framework (**j**). RCP 8.5 in 10-year influential time framework (**k**). RCP 8.5 in 15-year influential time framework (**l**)
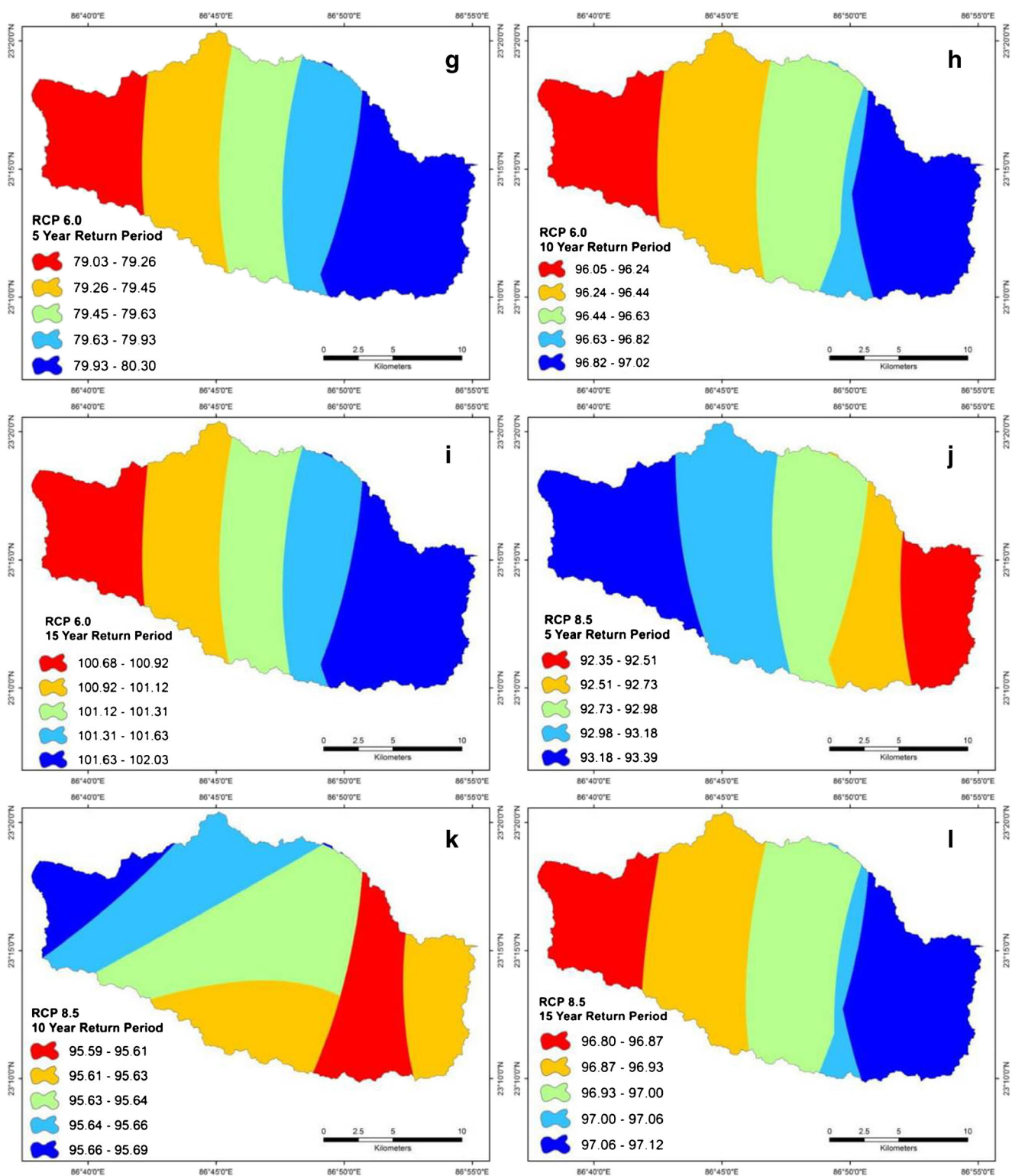
Fig. 9 (continued)

differences in this perspective. Pixel-wise information on the amount of soil loss is helpful to planners in taking the development strategy initiative. Special consideration must be given to the affected areas by the planners for

minimizing the amount of soil loss. Loss of soils alters the decline in soil fertility and the degradation of soil resources in the region. Some local support practices have been adopted by local stakeholders in order to minimize

Fig. 10 Future prediction of soil erosion. RCP 2.6 in 5-year influential time framework (**a**). RCP 2.6 in 10-year influential time framework (**b**). RCP 2.6 in 15-year influential time framework (**c**). RCP 4.5 in 5-year influential time framework (**d**). RCP 4.5 in 10-year influential time framework (**e**). 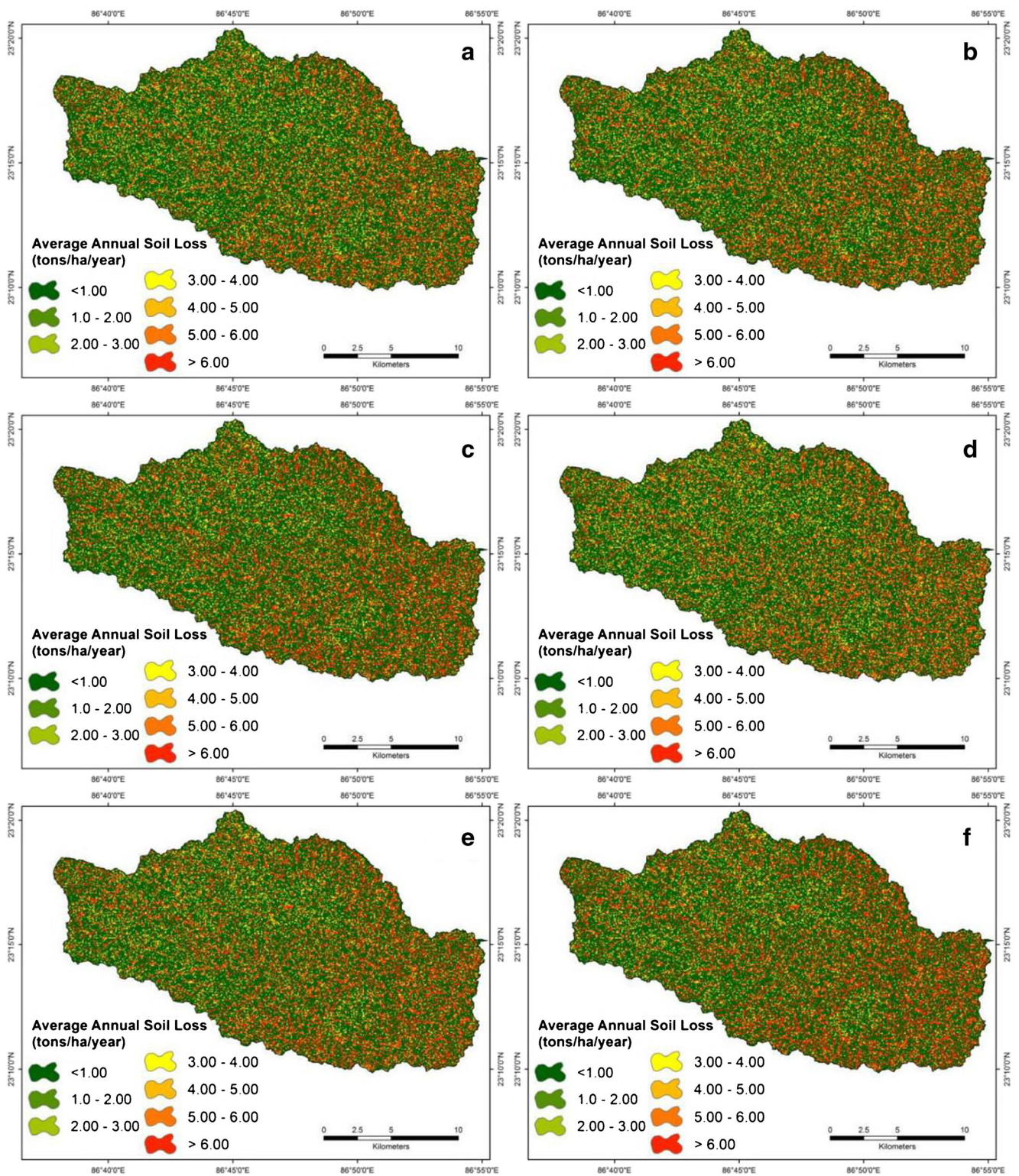RCP 4.5 in 15-year influential time framework (**f**). RCP 6.0 in 5-year influential time framework (**g**). RCP 6.0 in 10-year influential time framework (**h**). RCP 6.0 in 15-year influential time framework (**i**). RCP 8.5 in 5-year influential time framework (**j**). RCP 8.5 in 10-year influential time framework (**k**). RCP 8.5 in 15-year influential time framework (**l**)
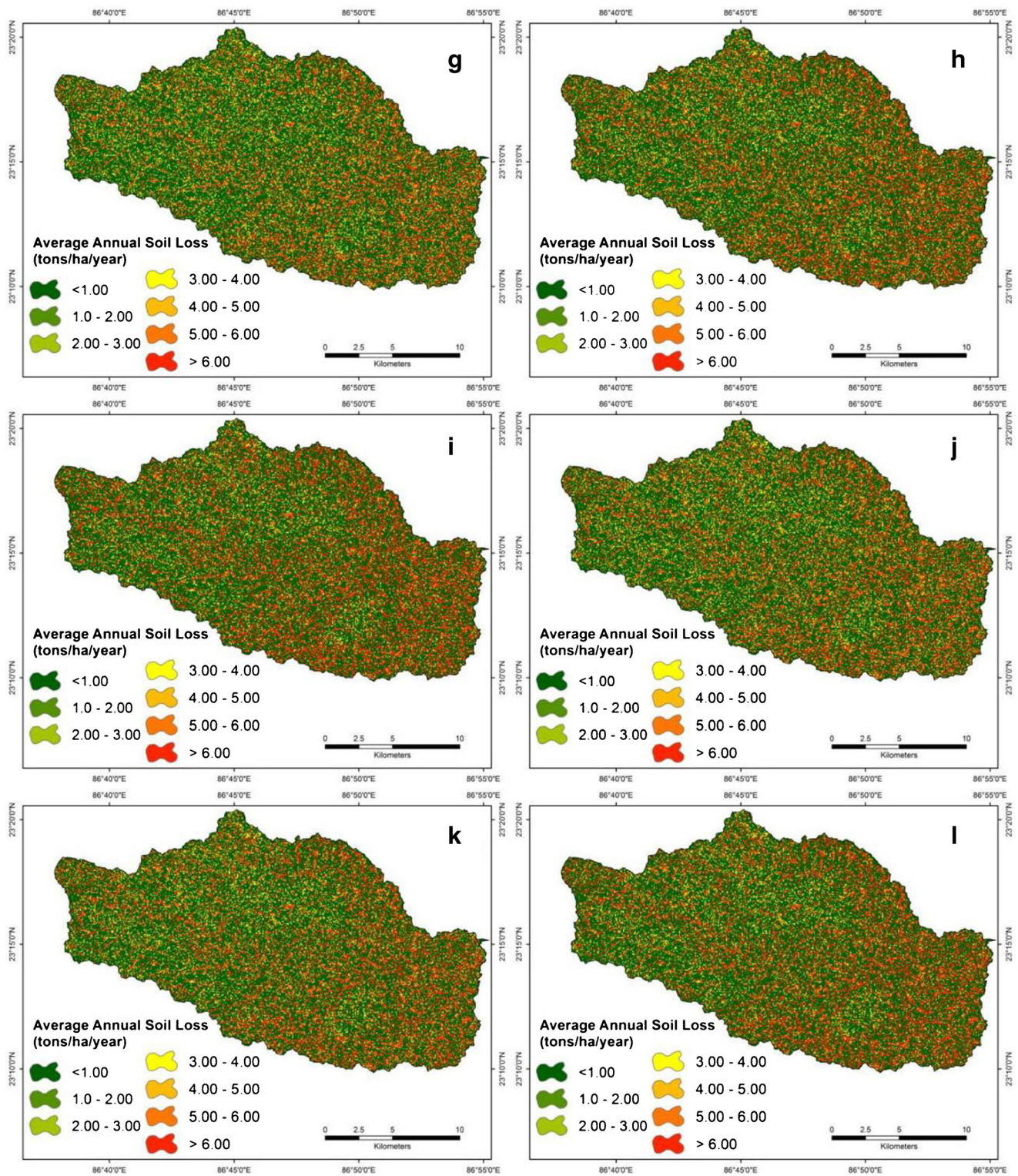
Fig. 10 (continued)

the impact of soil loss and to maintain soil fertility. Structural and non-structural measures must be taken in order to escape this kind of situation. Local governments and stakeholders have already taken some action to

reduce the loss of the top soil. However, as a result of this situation, such measures may not be appropriate to remedy the situation and may not comply with sustainable land management practices. Social forestry with external

Table 4 The rate of soil erosion and its spatial coverage in the future period

	5-year return period				10-year return period				15-year return period			
	Class name	Class range (ton/ha/year)	Area in hectare	Area in %	Class name	Class range (ton/ha/year)	Area in hectare	Area in %	Class name	Class Range (ton/ha/year)	Area in hectare	Area in %
RCP 2.6												
Average annual soil loss	Very high	> 6.00	1652.39	4.74	Very High	> 6.00	1846.30	5.30	Very High	> 6.00	1946.30	5.58
	High	5.00–6.00	3198.52	9.18	High	5.00–6.00	3312.60	9.50	High	5.00–6.00	3332.60	9.56
	Moderately high	4.00–5.00	2991.56	8.58	Moderately High	4.00–5.00	3820.00	10.96	Moderately High	4.00–5.00	3831.00	10.99
	Moderate	3.00–4.00	3341.55	9.59	Moderate	3.00–4.00	3431.00	9.84	Moderate	3.00–4.00	3421.00	9.82
	Moderately low	2.00–3.00	2953.53	8.47	Moderately Low	2.00–3.00	3263.50	9.36	Moderately Low	2.00–3.00	3363.50	9.65
	Low	1.00–2.00	3155.24	9.05	Low	1.00–2.00	3100.00	8.89	Low	1.00–2.00	3112.00	8.93
	Very low	< 1.00	17,559.21	50.38	Very Low	< 1.00	16,078.60	46.13	Very Low	< 1.00	15,845.60	45.47
Total			34,852.00	100.00	Total		34,852.00	100.00	Total		34,852.00	100.00
RCP 4.5												
Average annual soil loss	Very high	> 6.00	2046.30	5.87	Very high	> 6.00	2068.10	5.93	Very high	> 6.00	2102.00	6.03
	High	5.00–6.00	3340.60	9.59	High	5.00–6.00	3380.80	9.70	High	5.00–6.00	3410.20	9.78
	Moderately high	4.00–5.00	3890.00	11.16	Moderately high	4.00–5.00	3950.00	11.33	Moderately high	4.00–5.00	3980.00	11.42
	Moderate	3.00–4.00	3921.00	11.25	Moderate	3.00–4.00	4021.00	11.54	Moderate	3.00–4.00	4034.80	11.58
	Moderately low	2.00–3.00	3263.50	9.36	Moderately low	2.00–3.00	3213.50	9.22	Moderately low	2.00–3.00	3204.10	9.19
	Low	1.00–2.00	3211.00	9.21	Low	1.00–2.00	3190.00	9.15	Low	1.00–2.00	3110.50	8.92
	Very low	< 1.00	15,179.60	43.55	Very low	< 1.00	15,028.60	43.12	Very low	< 1.00	15,010.40	43.07
Total			34,852.00	100.00	Total		34,852.00	100.00	Total		34,852.00	100.00
RCP 6.0												
Average annual soil loss	Very high	> 6.00	1653.39	4.74	Very high	> 6.00	2069.10	5.94	Very high	> 6.00	2202.00	6.32
	High	5.00–6.00	3208.52	9.21	High	5.00–6.00	3383.80	9.71	High	5.00–6.00	3380.20	9.70
	Moderately high	4.00–5.00	2934.56	8.42	Moderately high	4.00–5.00	3948.00	11.33	Moderately high	4.00–5.00	4032.00	11.57
	Moderate	3.00–4.00	3343.55	9.59	Moderate	3.00–4.00	4020.30	11.54	Moderate	3.00–4.00	4012.80	11.51
	Moderately low	2.00–3.00	2953.53	8.47	Moderately low	2.00–3.00	3213.80	9.22	Moderately low	2.00–3.00	3204.10	9.19
	Low	1.00–2.00	3165.24	9.08	Low	1.00–2.00	3190.00	9.15	Low	1.00–2.00	3015.50	8.65
	Very low	< 1.00	17,593.21	50.48	Very low	< 1.00	15,027.00	43.12	Very low	< 1.00	15,005.40	43.05
Total			34,852.00	100.00	Total		34,852.00	100.00	Total		34,852.00	100.00
RCP 8.5												
Average annual soil loss	Very High	> 6.00	2969.10	8.52	Very high	> 6.00	3132.10	8.99	Very high	> 6.00	2182.50	6.26
	High	5.00–6.00	3283.80	9.42	High	5.00–6.00	3373.80	9.68	High	5.00–6.00	3288.20	9.43
	Moderately high	4.00–5.00	3948.00	11.33	Moderately high	4.00–5.00	4152.56	11.91	Moderately high	4.00–5.00	3932.50	11.28
	Moderate	3.00–4.00	3920.30	11.25	Moderate	3.00–4.00	4210.30	12.08	Moderate	3.00–4.00	4022.80	11.54

Table 4 (continued)

	5-year return period				10-year return period				15-year return period			
	Class name	Class range (ton/ha/year)	Area in hectare	Area in %	Class name	Class range (ton/ha/year)	Area in hectare	Area in %	Class name	Class Range (ton/ha/year)	Area in hectare	Area in %
	Moderately low	2.00–3.00	3313.80	9.51	Moderately low	2.00–3.00	3013.84	8.65	Moderately low	2.00–3.00	3204.10	9.19
	Low	1.00–2.00	2990.00	8.58	Low	1.00–2.00	3190.00	9.15	Low	1.00–2.00	3215.50	9.23
	Very low	<1.00	14,427.00	41.40	very low	<1.00	13,779.40	39.54	Very low	<1.00	15,006.40	43.06
Total			34,852.00	100.00	Total		34,852.00	100.00	Total		34,852.00	100.00

plant species has already been introduced, but this practice has become a false security for the protection of the upper soil. After considering the local indigenous spices, vegetative measures need to be taken. This type of data set generation information is effective and useful in the tropical and subtropical environments. It can be used for educational purposes as well as future soil loss research in the watershed area. Obviously, this type of data and its relevant information will help the civil engineer and planner to select the appropriate location of the reservoir and check the dam, the percolation tank, and so on.

Compliance with ethical standards

Competing interests The authors declare that they have no competing interests.

References

Abu Hammad A (2011) Watershed erosion risk assessment and management utilizing revised universal soil loss equation-geographic information systems in the Mediterranean environments: watershed erosion risk assessment in the Mediterranean environments. Water and Environment Journal 25:149–162. https://doi.org/10.1111/j.1747-6593.2009.00202.x

Arabameri A, Tiefenbacher JP, Blaschke T, Pradhan B, Tien Bui D (2020) Morphometric analysis for soil erosion susceptibility mapping using novel GIS-based ensemble model. Remote Sensing 12: 874. https://doi.org/10.3390/rs12050874

Arnoldus H (1980) An approximation of the rainfall factor in the universal soil loss equation. An approximation of the rainfall factor in the universal soil loss equation 127–132

Bera A (2017) Assessment of soil loss by universal soil loss equation (USLE) model using GIS techniques: a case study of Gumti River Basin, Tripura, India. Model Earth Syst Environ 3:29. https://doi.org/10.1007/s40808-017-0289-9

Biswas SS, Pani P (2015) Estimation of soil erosion using RUSLE and GIS techniques: a case study of Barakar River basin, Jharkhand, India. Model Earth Syst Environ 1:42. https://doi.org/10.1007/s40808-015-0040-3

Blaikie P (2016) The political economy of soil erosion in developing countries, 0 edn. Routledge

Carley M, Christie I (2017) Managing sustainable development, 2nd edn. Routledge

Chakrabortty R, Ghosh S, Pal SC et al (2018) Morphometric analysis for hydrological assessment using remote sensing and GIS technique: a case study of Dwarkeswar River Basin of Bankura District, West Bengal. Asia Jour Rese Soci Scie and Human 8:113. https://doi.org/10.5958/2249-7315.2018.00074.6

Chakrabortty R, Pal SC, Sahana M, Mondal A, Dou J, Pham BT, Yunus AP (2020) Soil erosion potential hotspot zone identification using

machine learning and statistical approaches in eastern India. Nat Hazards. https://doi.org/10.1007/s11069-020-04213-3

De Baets S, Poesen J, Gyssels G, Knapen A (2006) Effects of grass roots on the erodibility of topsoils during concentrated flow. Geomorphology 76:54–67. https://doi.org/10.1016/j.geomorph.2005.10.002

Edwards W, Owens L (1991) Large storm effects on total soil erosion. Journal of Soil and water Conservation 46:75–78

Ganasri BP, Ramesh H (2016) Assessment of soil erosion by RUSLE model using remote sensing and GIS-a case study of Nethravathi Basin. Geoscience Frontiers 7:953–961. https://doi.org/10.1016/j.gsf.2015.10.007

Gebremichael D, Nyssen J, Poesen J, Deckers J, Haile M, Govers G, Moeyersons J (2005) Effectiveness of stone bunds in controlling soil erosion on cropland in the Tigray Highlands, northern Ethiopia. Soil Use & Management 21:287–297. https://doi.org/10.1111/j.1475-2743.2005.tb00401.x

Gomez J, Sobrinho T, Giraldez J, Fereres E (2009) Soil management effects on runoff, erosion and soil properties in an olive grove of southern Spain. Soil and Tillage Research 102:5–13. https://doi.org/10.1016/j.still.2008.05.005

Gupta S, Kumar S (2017) Simulating climate change impact on soil erosion using RUSLE model−a case study in a watershed of mid-Himalayan landscape. J Earth Syst Sci 126:43. https://doi.org/10.1007/s12040-017-0823-1

Hembram TK, Saha S (2020) Prioritization of sub-watersheds for soil erosion based on morphometric attributes using fuzzy AHP and compound factor in Jainti River basin, Jharkhand, eastern India. Environ Dev Sustain 22:1241–1268. https://doi.org/10.1007/s10668-018-0247-3

Karaburun A (2010) Estimation of C factor for soil erosion modeling using NDVI in Buyukcekmece watershed. Ozean journal of applied sciences 3:77–85

Keesstra S, Mol G, de Leeuw J, Okx J, Molenaar C, de Cleen M, Visser S (2018) Soil-related sustainable development goals: four concepts to make land degradation neutrality and restoration work. Land 7:133. https://doi.org/10.3390/land7040133

Kouli M, Soupios P, Vallianatos F (2009) Soil erosion prediction using the revised universal soil loss equation (RUSLE) in a GIS framework, Chania, Northwestern Crete, Greece. Environ Geol 57:483–497. https://doi.org/10.1007/s00254-008-1318-9

Kumar S (2019) Geospatial approach in modeling soil erosion processes in predicting soil erosion and nutrient loss in hilly and mountainous landscape. In: Navalgund RR, Kumar AS, Nandy S (eds) Remote sensing of northwest Himalayan ecosystems. Springer Singapore, Singapore, pp 355–380

Lal R (2001) Soil degradation by erosion. Land Degrad Dev 12:519–539. https://doi.org/10.1002/ldr.472

Lal R (2005) Soil erosion and carbon dynamics. Soil and Tillage Research 81:137–142. https://doi.org/10.1016/j.still.2004.09.002

Lal R (2017) Soil erosion by wind and water: problems and prospects. In: Soil Erosion Research Methods, 2nd edn. Routledge, pp 1–10

Lane LJ, Hernandez M, Nichols M (1997) Processes controlling sediment yield from watersheds as functions of spatial scale. Environmental Modelling & Software 12:355–369. https://doi.org/10.1016/S1364-8152(97)00027-3

Malik S, Pal SC, Das B, Chakrabortty R (2019) Intra-annual variations of vegetation status in a sub-tropical deciduous forest-dominated area using geospatial approach: a case study of Sali watershed, Bankura, West Bengal, India. Geology, Ecology, and Landscapes 1–12

Malik S, Pal SC, Sattar A, Singh SK, Das B, Chakrabortty R, Mohammad P (2020) Trend of extreme rainfall events using suitable global circulation model to combat the water logging condition in Kolkata Metropolitan Area. Urban Climate 32:100599. https://doi.org/10.1016/j.uclim.2020.100599

Mishra BK, Rafiei Emam A, Masago Y, Kumar P, Regmi RK, Fukushi K (2018) Assessment of future flood inundations under climate and land use change scenarios in the Ciliwung River Basin, Jakarta. Journal of Flood Risk Management. 11:S1105–S1115. https://doi.org/10.1111/jfr3.12311

Moore ID, Burch GJ (1986) Physical basis of the length-slope factor in the universal soil loss equation. Soil Science Society of America Journal 50:1294–1298. https://doi.org/10.2136/sssaj1986.03615995005000050042x

Morgan R, Quinton J, Smith R et al (1998) The European soil erosion model (EUROSEM): a dynamic approach for predicting sediment transport from fields and small catchments. Earth Surface Processes and Landforms: The Journal of the British Geomorphological Group 23:527–544

Neave M, Rayburg S (2007) A field investigation into the effects of progressive rainfall-induced soil seal and crust development on runoff and erosion rates: the impact of surface cover. Geomorphology 87:378–390. https://doi.org/10.1016/j.geomorph.2006.10.007

Nyaupane N, Mote SR, Bhandari M, et al (2018) Rainfall-runoff simulation using climate change based precipitation prediction in HEC-HMS Model for Irwin Creek, Charlotte, North Carolina. In: World Environmental and Water Resources Congress 2018: Watershed Management, Irrigation and Drainage, and Water Resources Planning and Management - Selected Papers from the World Environmental and Water Resources Congress 2018

Oldeman LR, Hakkeling R, Sombroek WG (1990) World map of the status of human-induced soil degradation: an explanatory note. International Soil Reference and Information Centre

Pal S (2016) Identification of soil erosion vulnerable areas in Chandrabhaga river basin: a multi-criteria decision approach. Model Earth Syst Environ 2:5. https://doi.org/10.1007/s40808-015-0052-z

Pal SC, Chakrabortty R (2019a) Modeling of water induced surface soil erosion and the potential risk zone prediction in a sub-tropical watershed of eastern India. Modeling Earth Systems and Environment 5:369–393

Pal SC, Chakrabortty R (2019b) Simulating the impact of climate change on soil erosion in sub-tropical monsoon dominated watershed based on RUSLE, SCS runoff and MIROC5 climatic model. Advances in Space Research 64:352–377

Pal SC, Shit M (2017) Application of RUSLE model for soil loss estimation of Jaipanda watershed, West Bengal. Spatial Information Research 25:399–409

Pal SC, Chakrabortty R, Malik S, Das B (2018) Application of forest canopy density model for forest cover mapping using LISS-IV satellite data: a case study of Sali watershed, West Bengal. Model Earth Syst Environ 4:853–865. https://doi.org/10.1007/s40808-018-0445-x

Panagos P, Karydas CG, Gitas IZ, Montanarella L (2012) Monthly soil erosion monitoring based on remotely sensed biophysical parameters: a case study in Strymonas river basin towards a functional pan-European service. International Journal of Digital Earth 5:461–487. https://doi.org/10.1080/17538947.2011.587897

Panagos P, Borrelli P, Meusburger K (2015) A new European slope length and steepness factor (LS-factor) for modeling soil erosion by water. Geosciences 5:117–126. https://doi.org/10.3390/geosciences5020117

Pimentel D (2006) Soil erosion: a food and environmental threat. Environ Dev Sustain 8:119–137. https://doi.org/10.1007/s10668-005-1262-8

Plangoen P, Babel M, Clemente R, Shrestha S, Tripathi N (2013) Simulating the impact of future land use and climate change on soil erosion and deposition in the Mae Nam Nan sub-catchment, Thailand. Sustainability 5:3244–3274. https://doi.org/10.3390/su5083244

Prasannakumar V, Vijith H, Abinod S, Geetha N (2012) Estimation of soil erosion risk within a small mountainous sub-watershed in Kerala, India, using revised universal soil loss equation (RUSLE) and geo-information technology. Geoscience Frontiers 3:209–215. https://doi.org/10.1016/j.gsf.2011.11.003

Renard KG, USA, USA (eds) (1997) Predicting soil erosion by water: a guide to conservation planning with the revised universal soil loss equation (RUSLE), Washington, D. C

Rouse Jr J (1974) Monitoring the vernal advancement and retrogradation (green wave effect) of natural vegetation

Roy P, Chakrabortty R, Chowdhuri I, Malik S, Das B, Pal SC (2020a) Development of different machine learning ensemble classifier for gully erosion susceptibility in Gandheswari Watershed of West Bengal, India. In: Rout JK, Rout M, Das H (eds) Machine Learning for Intelligent Decision Science. Springer Singapore, Singapore, pp 1–26

Roy P, Pal SC, Chakrabortty R et al (2020b) Threats of climate and land use change on future flood susceptibility. Journal of Cleaner Production 122757

Saha A, Ghosh M, Pal SC (2020) Gully Erosion Studies from India and Surrounding Regions. In: Understanding the morphology and development of a rill-gully: an empirical study of Khoai Badland, West Bengal, India. Springer, In, pp 147–161

Senanayake S, Pradhan B, Huete A, Brennan J (2020) Assessing soil erosion hazards using land-use change and landslide frequency ratio method: a case study of Sabaragamuwa Province, Sri Lanka. Remote Sensing 12:1483

Shit P, Bhunia G, Maiti R (2015) Farmers' perceptions of soil erosion and management strategies in South Bengal in India. European Journal of Geography 6:85–100

Shrestha S, Lohpaisankrit W (2017) Flood hazard assessment under climate change scenarios in the Yang River Basin, Thailand. International Journal of Sustainable Built Environment. 6:285–298. https://doi.org/10.1016/j.ijsbe.2016.09.006

Stoorvogel JJ, Bakkenes M, Temme AJAM, Batjes NH, Brink BJE (2017) S-world: a global soil map for environmental modelling. Land Degrad Develop 28:22–33. https://doi.org/10.1002/ldr.2656

Teng H, Liang Z, Chen S, Liu Y, Viscarra Rossel RA, Chappell A, Yu W, Shi Z (2018) Current and future assessments of soil erosion by water on the Tibetan Plateau based on RUSLE and CMIP5 climate models. Science of The Total Environment 635:673–686. https://doi.org/10.1016/j.scitotenv.2018.04.146

Thomas J, Joseph S, Thrivikramji KP (2018) Assessment of soil erosion in a tropical mountain river basin of the southern Western Ghats, India using RUSLE and GIS. Geoscience Frontiers 9:893–906. https://doi.org/10.1016/j.gsf.2017.05.011

Tiwari H, Rai SP, Kumar D, Sharma N (2016) Rainfall erosivity factor for India using modified Fourier index. Journal of Applied Water Engineering and Research 4:83–91. https://doi.org/10.1080/23249676.2015.1064038

Toubal AK, Achite M, Ouillon S, Dehni A (2018) Soil erodibility mapping using the RUSLE model to prioritize erosion control in the Wadi Sahouat basin, north-west of Algeria. Environ Monit Assess 190:210. https://doi.org/10.1007/s10661-018-6580-z

Van der Knijff J, Jones R, Montanarella L (2000) Soil erosion risk assessment in Europe, EUR 19044 EN. Office for official publications of the European communities, Luxembourg 34

Van Remortel RD, Maichle RW, Hickey RJ (2004) Computing the LS factor for the revised universal soil loss equation through array-based slope processing of digital elevation data using a C++ executable. Computers & geosciences 30:1043–1053

Van Romortel R, Hamilton M, Hickey R (2001) Estimating the LS factor for RUSLE through iterative slope length processing of digital elevation data within ArcInfo grid. Cartography 30:27–35

Wang X, Li Z, Cai C, Shi Z, Xu Q, Fu Z, Guo Z (2012) Effects of rock fragment cover on hydrological response and soil loss from Regosols in a semi-humid environment in South-West China. Geomorphology 151–152:234–242. https://doi.org/10.1016/j.geomorph.2012.02.008

Wischmeier WH (1978) Predicting rainfall erosion losses. USDA agricultural research services handbook 537

Wischmeier WH, Smith DD (1958) Rainfall energy and its relationship to soil loss. Trans AGU 39:285. https://doi.org/10.1029/TR039i002p00285

Wischmeier WH, Johnson C, Cross V (1971) A soil erodibility nomograph forfarmland and construction sites. Journal of Soil and Water Conservation 26(5):189–193

Yang D, Kanae S, Oki T, Koike T, Musiake K (2003) Global potential soil erosion with reference to land use and climate changes. Hydrol Process 17:2913–2928. https://doi.org/10.1002/hyp.1441

Zeng C, Wang S, Bai X, Li Y, Tian Y, Li Y, Wu L, Luo G (2017) Soil erosion evolution and spatial correlation analysis in a typical karst geomorphology using RUSLE with GIS. Solid Earth 8:721–736. https://doi.org/10.5194/se-8-721-2017

Zhang XC, Nearing MA (2005) Impact of climate change on soil erosion, runoff, and wheat productivity in central Oklahoma. Catena 61:185–195

Zhou P, Luukkanen O, Tokola T, Nieminen J (2008) Effect of vegetation cover on soil erosion in a mountainous watershed. CATENA 75:319–325. https://doi.org/10.1016/j.catena.2008.07.010